Aeromagnetic Modeling of the Sudbury Structure's South Range: Presence of a Central Uplift?

by

Sebastián Guardo Cardona

Thesis Report, Submitted in Partial Fulfillment of the Requirements for the Degree of **Geologist**

Supervisor:

Hernan Ugalde, Ph.D., P.Geo.

EAFIT University
School of Applied Sciences and Engineering
Geology
Medellín, Colombia

2023

To my father, **Gustavo**, for his inspiration.

To my mother, **Chachi**, for the early wake-ups.

To my partner in crime, **Ali**, for her care.

To **Dora** and **Ana**, for all their love.

Acknowledgments

The realization of this thesis would not be possible without the inspiration and collaboration of the following people:

Professor Hernan Ugalde, my mentor in the development of this project and my official vegetable supplier.

Professor William “Bill” Morris, the voice of wisdom.

Professors linked to the Geology program of EAFIT University, especially Isabel Restrepo for showing me the beauty of geophysics, and Juan "Pani" Paniagua for pushing me with his energy.

To my fellow partners, especially the ones of The Last Supper, for all the intoxicated nights in *La Carpita Roja*.

Content

s

Abstract

The Sudbury Structure (SS) is an impact crater in Northern Ontario (Canada), known for its significant concentrations of sulfide ores and the complexity of its structural setting. Even after decades of research and exploration, essential questions about its basin structural arrangement remain unresolved. One of these unsolved problems is the existence of the impact crater's central uplift, a structure that, if recognized, might improve the understanding of the Sudbury Structure's geological history and its mineral deposit arrangement. Here, we evaluated whether the SS's South Range could house the Structure's central uplift. A 3D model of the SS's South Range's central zone using magnetic and structural data is presented here to evaluate the presence of the central uplift within this area. We identified a dome-shaped structure on the model's lower noritic surface, accompanied by a horizontalizing behavior on the model's upper overlaying surfaces. By comparing the observed modeled structural disposition with a conceptual model representing a present central uplift scenario, we propose the presence of this structure in the SS's South Range's central zone. This consideration might help to clarify Sudbury Structure subsurface rocks disposition relating some of its main magnetic and structural characteristics to the final modeled surfaces' magnetic values and geometrical tendencies.

Keywords: Sudbury Structure, South Range, Central Uplift, Impact Crater, 3D Model.

1. Introduction

The Sudbury Structure of the Canadian Shield is an Early Proterozoic impact crater in Northern Ontario, Canada (Figure 1) that has undergone many phases of deformation. Its Northern, Eastern, and Southern sides (known as "Ranges") all show different magnetic patterns that could help define the geometry of the basin (Card et al., 1984). Despite being recognized for over a century for its significant concentrations of sulfide ores, the complexity of its structural setting, and decades of research and exploration (Giblin, 1984), essential questions about the Sudbury Structure's structural arrangement remain unresolved.

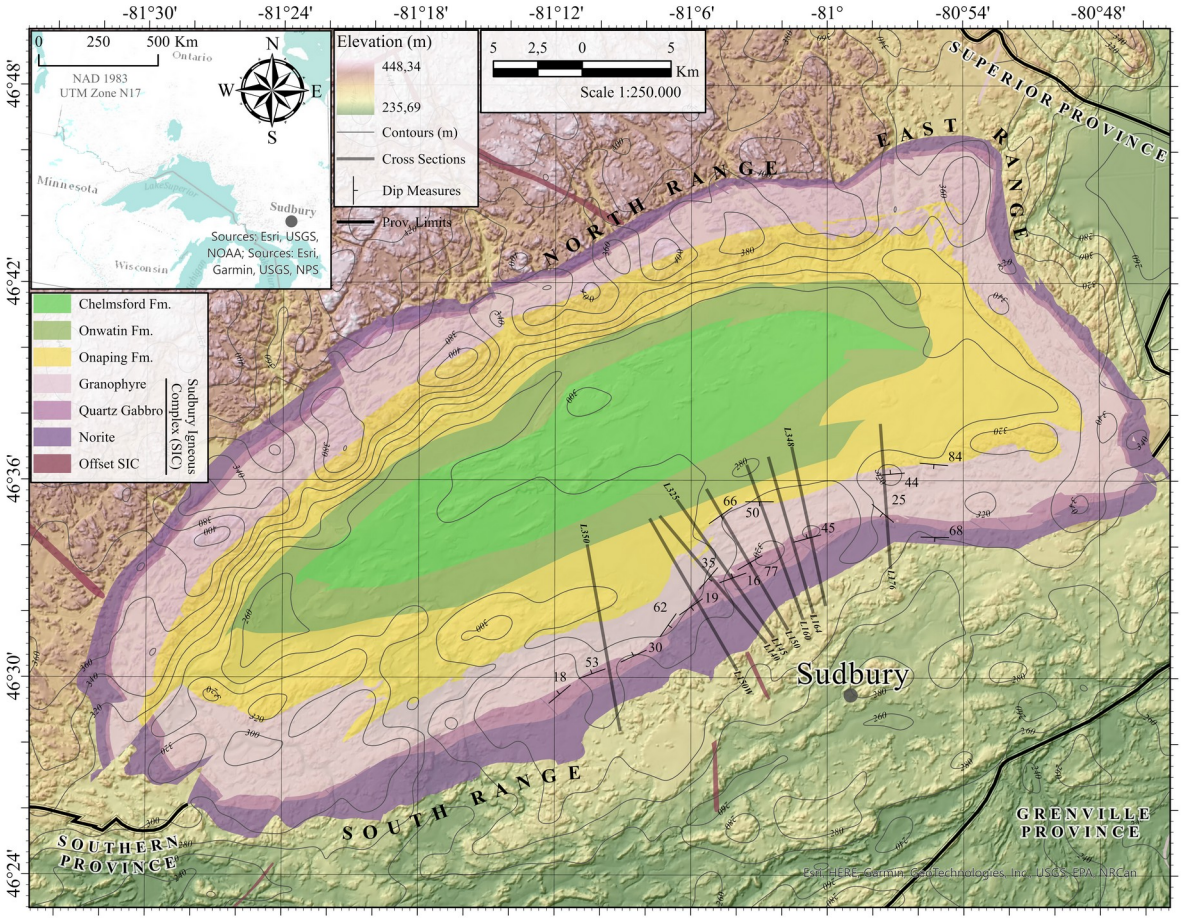

Figure 1. Geology of the Sudbury Basin. Cross-sections used for modeling have been highlighted. Own elaboration using Ontario Geological Survey (2023) data.

One of these unsolved questions is the setting of its central uplift, a dome-shaped structure inherent to any complex impact crater (Kenkmann et al., 2005; Morris et al., 2022), and that might be crucial for understanding the geological history and possibly mineral deposit arrangement of the Sudbury Structure (SS). Over the years, it has been

proposed the formation and subsequent subsidence of the central uplift of the SS (French, 1967, 1972, as cited in Rousell, 1984); it has also been suggested its collapse after the set-up of the Sudbury Igneous Complex (SIC), another crucial structure of the SS (Peredery & Morrison, 1984). Its former presence and possible extent have also been proposed as part of a geological history reconstruction of the basin (Spray et al., 2004, as cited in Riller, 2005). Even so, the central uplift's current location and extent still need to be clarified. Understanding the structural arrangement of the subsurface can help better comprehend its structural setting and grasp an adequate understanding of the basin's geological history.

A three-dimensional model of the more magnetic strata of the Southern Range of the structure, made using aeromagnetic (Olaniyan et al., 2013), inferred structural (Dreuse et al., 2010; Lenauer & Riller, 2012), and existing susceptibility magnetic data (Card et al., 1984; Gupta et al., 1984; Ontario Geological Survey, 2023), is presented here to postulate the location of the central uplift in the Southern Range of the basin. This should help to improve the understanding of the origin and emplacement of the Sudbury Crater and might suggest a new location of interest for further ore exploration in the basin.

2. Basic Concepts

2.1. Research Inquiry

Is there a central uplift in the Sudbury Structure? If yes, could it be identified in the basin's South Range?

2.2. Hypothesis

The Sudbury Structure's South Range houses the impact crater's central uplift.

2.3. Objective

Create a 3D model of the Sudbury Structure's South Range using aeromagnetic and structural data, and evaluate whether this structural model supports the presence of a central uplift.

2.4. Specific Objectives

- Gather the magnetic and ancillary structural data available for the South Range of the Sudbury Structure.
- Create several 2D cross-section models to create a subsurface 3D model per the previously gathered data.
- Interpret the 3D structural model and see whether the central uplift is supported.

3. Geological Setting

The location area of the Sudbury Structure is situated at the contact junction between three main geological subdivisions of the Canadian Shield: Superior, Southern, and Grenville Provinces (Dressler, 1984). It is outlined by the Sudbury Igneous Complex (1.85 Ga), one of the most highly mineralized bodies in the entire Canadian Shield (Percival & Easton, 2007), of particular interest due to its structural complexity and the great abundance of its Ni-PGE deposits (Giblin, 1984).

3.1. Canadian Shield

The Canadian Shield (CS) is a peneplain surface conformed mainly by ancient crystalline rocks with over a billion years of geological history (Renwick, 2009; Britannica, 2023). It is subdivided into several structural provinces with very well-established boundaries where a structural trend is truncated by another, either along major unconformities or orogenic fronts (Stockwell, 1975). The principal Archean Provinces of the CS formed in the Eoarchean to Neoarchean, and they exhibit rich Neoarchean to early Paleoproterozoic deformation and metamorphism (Kellet et al., 2020).

The Sudbury Structure is located right at the limit between the Archean rocks of the Superior Province and the Early Proterozoic rocks of the Southern Province, approximately 10 km away from the northern limit of the Grenville Province, the Grenville Front (Figure 1).

3.1.1. Superior Province

The Superior Province covers a geological history from 3.6 Ga to 2.6 Ga (Percival & Easton, 2007). It can be considered as a composition of small continental and oceanic plates (Card, 1990; Williams et al., 1992; Stott, 1997; Percival et al., 2004; Percival et al., 2006, as in Percival & Easton, 2007). Five microcontinental fragments developed independently between 3.6-2.75 Ga, followed by five distinct accretionary events between 2.72-2.68 Ga that ultimately united the continental and intervening oceanic crustal domains into the present-day Superior craton (Percival & Easton, 2007).

The Sudbury Structure is situated in the eastern region of the Superior Province, in the Abitibi Terrane, a volcanic-rich Subprovince characterized by sinuous greenstone belts, upright folds, and domal structures (Card et al., 1984). Part of the Archean rocks of the

Abitibi Terrain consists of massive felsic plutons called the Algoman plutons (Card et al., 1984). The Abitibi Terrain has been subdivided into three principal domains: one up north made of volcanic assemblages (2.735-2.72 Ga) (Ludden et al., 1986; Chown et al., 1992; Legault et al., 2002, as in Percival & Easton, 2007) and layered intrusions (Percival & Easton, 2007); one central assemblage consisting mainly of plutonic rocks (Chown et al., 2002, as in Percival & Easton, 2007); and another southern assemblage consisting of volcanic rocks (2.71-2.695 Ga) (Dimroth et al., 1984; Daigneault et al., 2002, as in Percival & Easton, 2007) and sedimentary-volcanic deposits (ca. 2.69 Ga), along with conglomeratic and alkaline volcanic rocks (2.677-2.673 Ga) (Davis, 2002, as in Percival & Easton, 2007).

3.1.2. Southern Province

The Southern Province is known as the most antique sequence on the margin of the Superior Province (Bennett et al., 1991; Long, 2004, as in Percival & Easton, 2007), subdivided mainly in two: the Penokean fold belt in the west and gently folded rocks of the Cobalt embayment in the east (Percival & Easton, 2007).

A discontinuous linear fold belt of around 1300 km long, made up of Early Proterozoic supracrustal rocks of the Southern Province (Huronian Supergroup in the east, Marquette Range Supergroup, and Animikie Group in the west), crosses the southern margin of the Superior Province (Card et al., 1972, as in Card et al., 1984).

The sequences were deposited around 2.5 and 1.9 million years ago. They are mainly composed of clastic sedimentary rocks and volcanic rocks, with a smaller amount of chemical sedimentary rocks, particularly iron formation. The Huronian Supergroup consists principally of glaciomarine to fluvio-deltaic sedimentary sequences. These clastic sedimentary rocks came from the Archean craton of the Superior Province to the north (Card et al., 1984).

The Elliot Lake Group is the basal unit of the Southern Province. It consists of a mixed ensemble of sedimentary and volcanic rocks (Card et al., 1984). The Skead (2.47 Ga), Murray (2.47 Ga), and Creighton plutons (2.41-2.37 Ga) can be found intruded into the basal volcanic units of the Elliot Lake Group (Percival & Easton, 2007).

3.1.3. Grenville Province

The Grenville Province is a gneissic terrain containing rocks ranging between 2.69-0.99 Ga, subjected to Grenvillian metamorphism (Percival & Easton, 2007). It borders the Superior and Southern provinces along its northern and western margins via the Grenville Front, recognized as an NE-trending zone (Card et al., 1984; Percival & Easton, 2007). The metamorphism grade in the Front goes from greenschist facies in the Southern Province limit to upper amphibolite facies in the Grenville Province, showing migmatites forming the Front's hanging wall (Percival & Easton, 2007).

3.2. Sudbury Structure

The Sudbury Structure, located at the southern limit of the Superior Province, is outlined by a differentiated sill of gabbroic-noritic composition with a granophyric top that forms an elliptical ring that is around 60 km long and 27 km wide (Dressler et al., 1991, as in Percival & Easton, 2007; Gupta et al., 1984). This intrusion of rocks is known as the Sudbury Igneous Complex (SIC) (1.85 Ga), one of the most highly mineralized bodies of the Canadian Shield, generated by crustal melting (Mungall et al., 2004, as in Percival & Easton, 2007) caused by a meteorite impact (Ames, 1999; Rousell et al., 2002; Therriault et al., 2002; Rousell et al., 2003; Ames et al., 2005, as in Percival & Easton, 2007).

3.2.1. Sudbury Igneous Complex

The form of the SIC can be described as an asymmetric, funnel-shaped body whose North Range dips moderately south, at approximately 45°S (to the center of the Sudbury Structure), and its South Range dips steeply northward, at around 65°N (Gupta et al., 1984; Lenauer & Riller, 2017). It embodies a synclinorial basin, i.e., the Sudbury Basin, made of breccias, mudstones, and wackes from the Whitewater Group. At the base of the Whitewater Group, the heterolithic lower breccias of the Onaping Formation are overlain by the mudstones of the Onwatin Formation, which are overlain by the turbiditic wackes of the Chelmsford Formation (Gupta et al., 1984).

The SIC lowermost unit is the Sublayer, a range of noritic, gabbroic, and quartz dioritic rocks that occur inside Sudbury Basin fractures (Naldrett, 1984). Up from this Sublayer, the SIC can be subdivided into three central regions: the Lower, Middle, and Upper Zones.

The Lower Zone of the SIC consists mainly of Noritic units that vary in composition along the Ranges of the Sudbury Structure. In the South Range, the Quartz-rich Norite constitutes the marginal zone that grades upward into the South Range Norite. On the other side of the Basin, the Mafic Norite occurs discontinuously along the North Range, overlain by the Felsic Norite, a petrographically equivalent to the top of the South Range Norite (Naldrett, 1984).

The Middle Zone of the SIC is made of a Quartz Gabbro unit that can be found around the basin. Fe-Ti oxides are common at the base of this unit, while in the South Range, magnetite and ilmenite occur, and in the North Range is the titaniferous magnetite that makes a presence with the Quartz Gabbro unit (Naldrett, 1984).

The Upper Zone of the SIC is delimited from the Middle Zone by increased granophyric intergrowth of quartz, plagioclase, and potassic feldspar. In this way, the Quartz Gabbro of the Middle Zone is overlain by a Granophyre unit, which contains approximately 75-85% of the intergrowth. A variant of this unit containing 40-50% plagioclase occurs at the top of the Upper Zone. This variant is known as the Plagioclase-rich Granophyre (Naldrett, 1984).

3.3. Sudbury Structure's Geophysical Characteristics

Interpreting geophysical data allows the identification of features in the subsurface. However, it should always be considered that this analysis can lead to different interpretations due to the intrinsic nature of the potential field signals emanated by the Earth's magnetic field and how these signals might be interpreted differently depending on the observer's analysis. Another limitation is that geophysical observations are usually dominated by shallow source information, which can mask the long wavelength signals associated with deeper source anomalies (Card et al., 1984).

Magnetic Susceptibility is the physical property that "relates a material's magnetization to the strength of an applied magnetic field" (Mugiraneza & Hallas, 2022). In the Sudbury Basin, the SIC's units constrain the higher susceptibility values encountered within the different rock units, with its highest peak being within the Noritic and Quartz-Gabbroic rocks that show an average magnetic susceptibility of 0,55 SI (Ontario Geological Survey, 2023). For a detailed view of the susceptibility values encountered in the SS and the ones used in this project, please refer to Section 5.1.

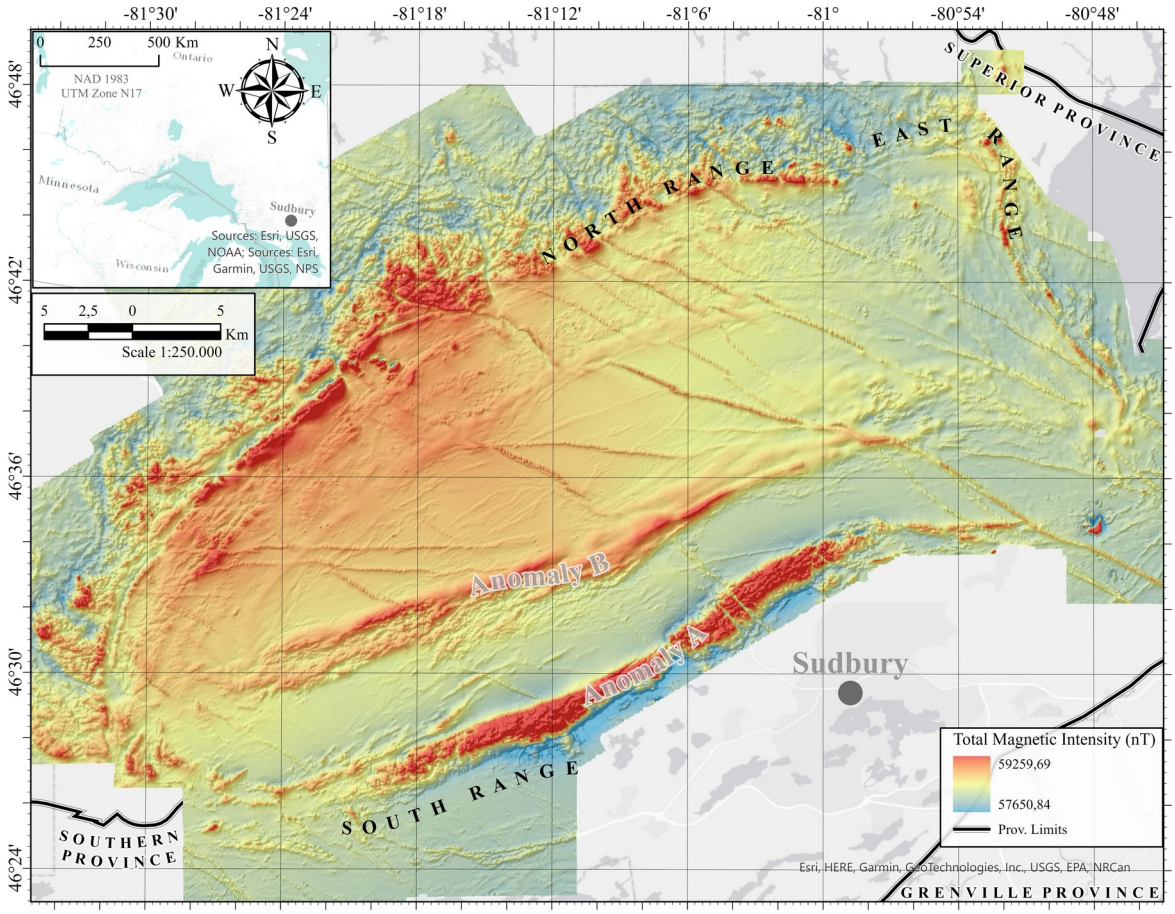

Figure 2. Total Magnetic Intensity of the Sudbury Basin. The main positive anomalies for the South Range (A and B anomalies) have been highlighted. Own elaboration using Olaniyan et al. (2013) data.

Observing the aeromagnetic map of the study area (Figure 2), it can be noticed that a very distinguishable oval-shaped anomaly delimits the Sudbury Structure (Gupta et al., 1984). Two main components can be identified within the basin's South Range of this prominent magnetic feature:

- Anomaly A: Coinciding with the SIC, there is a semicontinuous elliptic positive anomaly that, in the South Range, seems to be related to the Noritic bedrock units of the SIC (Figure 2). It can be noted how this anomaly presents a greater amplitude over the South Range of the Basin than over the North Range (Gupta et al., 1984).
- Anomaly B: Near the contact limit between the Onaping and Onwatin Formations in the South Range of the Basin, there is an almost linear, positive anomaly (Figure 2) whose origin is not certainly known but can be related to some intruded gabbroic units in the Onwatin Formation (Gupta et al., 1984).

4. Sudbury Structure's Impact Crater

An impact crater results from a cosmic projectile that enters Earth's atmosphere with minimal deceleration and collides with the ground at practically its initial cosmic velocity. These projectiles travel faster than the speed of sound when they strike and thus generate powerful shock waves that travel through the surrounding terrain, deforming the target surface and shaping the impact crater (French, 1998). These shock waves are intense, fleeting, high-pressure stress waves that can produce shock pressures of several hundred GPa, much higher stress levels than those experienced by terrestrial rocks in ordinary elastic and plastic deformation, and therefore producing unique and permanent deformation traces in the target rocks and surfaces they strike (French, 1998).

Over the years, many studies have discussed an impact origin for the Sudbury Basin (Dietz, 1964; Muir, 1984; Peredey & Morrison, 1984). Different attributes have been discovered that support this hypothesis. The shock metamorphic features encountered in the rock units of the Onaping Formation and the Sudbury Basin's Footwall (and the documented brecciation of the latter) (Dressler et al., 1987), as well as some geophysical signatures present in other impact structures like pronounced gravity lows, prominent magnetic anomalies, and the absence of prominent reflections in the crater's footwall, represent some of the evidence that supports an impact origin for the Sudbury Structure (Milkereit et al., 2008). Whether these characteristics support an impact or endogenic origin will not be further discussed in this article, as the impact origin can currently be considered the leading cause for the setting of the Sudbury Structure, as it has been previously demonstrated by different authors (Dence, 1972; Dietz, 1964; Dressler, 1984; Dressler et al., 1987; French, 1968; Guy-Bray & Geological Staff, 1966; French, 1970; French, 1972; Peredery, 1972; Morrison, 1984; Peredery & Morrison, 1984; Stüoffler et al., 1989, as in Dressler et al., 1992).

4.1. Impact Crater Formation

The process through which an impact crater reaches its final configuration can be divided into three stages, each characterized by its distinctive forces and mechanisms: contact and compression, excavation, and modification (Gault et al., 1968; Melosh, 1989, as in French, 1998). Now, the different stages through which an impact structure forms will be briefly described.

4.1.1. Contact and Compression

Once the projectile contacts the ground surface, shock waves expand into the target rocks as secondary shock waves reflect into the projectile (French, 1998). Equation 1 (French, 1998) describes how the pressures of the shock waves behave once they move away from the impact zone, where P_s is the peak shock wave pressure, and R is the distance from the impact zone.

Equation 1.
$P_s \boldsymbol{\alpha} R^{-n}$

In a nutshell, the values of P_s drop exponentially with the magnitude of R (French, 1998). The value of the R exponent relies on the projectile size and impact velocity, though several studies suggest a dependence *of* R^{-2} *to* $R^{-4.5}$ (Ahrens & O'Keefe, 1977, as in French, 1998). This relation (Equation 1) explains the different shock-metamorphic effects experimented by the target rocks according to their distance from the impact point. At the impact point, where P_s may be greater than 1000 GPa, vaporization and total melting of the surrounding target rocks and the projectile occur (French, 1998). Moving further from the impact point, P_s of 10–50 GPa extend along several kilometers, leaving shock-deformation traces in unmelted units of the target rock (French, 1998). Near the eventual crater rim, Ps values drop to 1-2 GPa (Kieffer and Simonds, 1980, as in French, 1998), and shock waves evolve into seismic waves that may generate fracturing, brecciation, faulting, and landslides in the rocks through which they pass (French, 1998). The contact and compression stage lasts only a few seconds before it grades into the more prolonged excavation stage.

4.1.2. Excavation and Modification

In this stage, the initial impact crater is "opened up by complex interactions between the expanding shock waves and the original ground surface*"* (Melosh, 1989; Grieve, 1991, as in French, 1998). Firstly, a hemispherical envelope of shock waves surrounds the projectile, expanding through the target rocks. The shock waves intersecting the original ground surface are reflected as rarefaction (release) waves, which fracture and shatter the target rock. This reflection turns some initial shock waves into kinetic energy that removes the impact surface material at high velocities, assembling a symmetric bowl-shaped

excavation flow near the center of the structure, the transient cavity (Figure 3) (French, 1998).

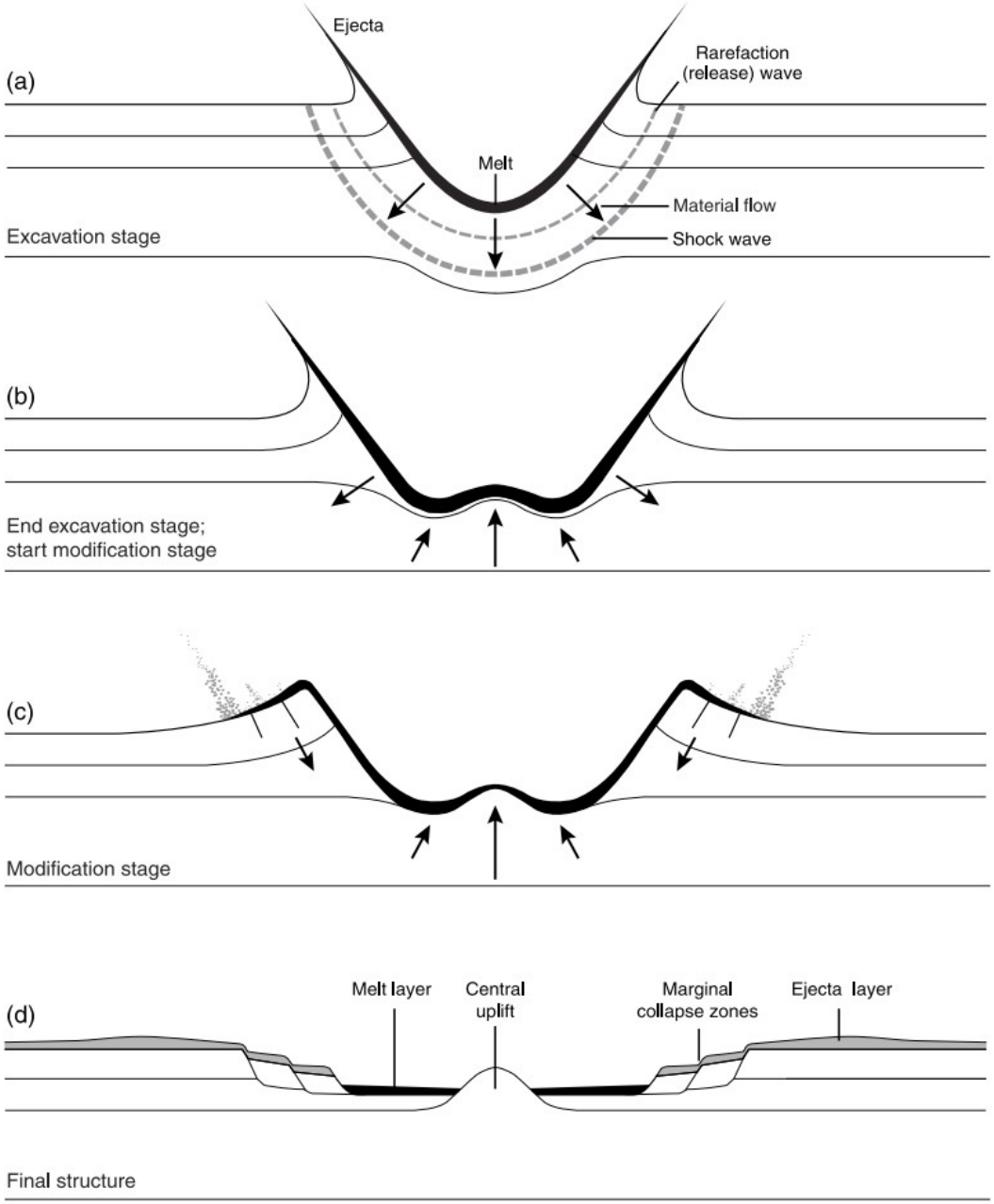

Figure 3. Excavation and modification stages of a complex impact structure. Taken from French (1998).

There is a brief moment of theoretical balance where the shock wave's energy stops, and the forces of gravity and rock mechanics have not taken over yet. During this moment, the transient cavity reaches its maximum size (the whole process can last from a few seconds to a couple of minutes), marking the end of the excavation stage and the start of the modification stage (French, 1998). At this stage, the expanding shock waves decay into

low-pressure elastic stress waves that go past the crater rim, no longer imperative in the crater evolution. From this point, the uplift and collapse of the target rocks in the transient cavity gradually merge into more common shape-defining processes like erosion and sedimentation (French, 1998).

4.2. Types of Impact Structures

The degree of alteration to the transient crater during the modification stage varies depending mainly on its size. Nevertheless, all impact structures present three principal features in common, irrespective of their extent. First, they have a nearly flat crater floor. Second, the crater wall inclines gradually towards the center of the crater. Lastly, the crater's rim is elevated, with rocks sloping away from the center or even appearing overturned (Morris et al., 2022). In the case of small transient craters, the upper walls may collapse, but the overall shape of the final crater tends to remain unaltered. Conversely, larger impact structures may undergo significant changes, like developing a central uplift or undergoing major peripheral collapse around the rim (French, 1998). Based on the degree of modification, impact structures can be categorized into three types: simple craters, complex craters, and multiring basins.

It is unclear which type of impact structure the SS originally was, though given the extent of its diameter (though it is still not clear its full extent, it is probably between the 200-250 km range) and the dimension of its SIC, it may represent the central portion of a grander complex-multiring crater (French, 1998; Morris et al., 2022). Nevertheless, it has also been suggested that the Sudbury impact structure might represent a peak-ring impact basin (a complex impact structure that forms a ring structure from its original central peak zone) (Riller, 2005). Establishing the extent and location of its presumed central uplift can help clarify the matter.

4.2.1. Simple and Complex Craters

Simple craters represent the smallest types of impact structures, extending less than a few kilometers; thus, its transient cavity's original dimensions and shape remain well preserved over time, modified only by minor collapse of its upper walls and by redeposition of ejected material into the crater (crater-fill breccia) (French, 1998). The progression from simple to complex craters in terrestrial structures is conditional upon the composition of the rock in which they are created. In the case of crystalline rocks, this transition takes place

around the 4 km mark in diameter, whereas in sedimentary rocks, it is at approximately 2 km. Complex craters are considerably larger impact structures than simple craters; they possess a more intricate shape, distinguished by a central uplifted area, a relatively flat floor, and extensive inward collapse around the rim (Dence, 1968; Grieve et al., 1977; Grieve et al., 1981; Grieve, 1991, as in French, 1998).

As a result of the significant impact of events that generate complex craters (capable of routing the strength and structure of the target rocks while involving shock waves and gravity), the modification of these impact structures is dominated by outward, inward, and upward motions of the subcrater rock units (French, 1998).

While the specifics of these interactions remain unclear, the main result is that the deep-seated rocks modify the transient cavity as they rise under the center of the crater, forming a central uplift (Figure 3) (Dence, 1968; Grieve et al., 1977; Grieve, 1991, as in French, 1998). Simultaneously, the rocks around the crater's perimeter collapse downwards and inwards along concentric faults, forming one or more ring grabens and a succession of terraces along the outer edges of the final crater (French, 1998).

Several studies suggest the presence of a central uplift in the Sudbury Structure. Prevec et al. (2005) proposed the presence of an impact-induced central uplift that might result from a post- or syn-impact uplift. Grieve and Therriault (2000) suggested that the SIC overlies a central uplift, as the target rocks are either younger or "up crust" away from the SIC. Milkereit et al. (2008), in a footwall's signature correlation of several impact structures, including Sudbury's, involved the presence of preheated rocks at a modeled central uplift. For the South Range of the Sudbury Structure, uplifting has been previously proposed by Gupta et al. (1984) and Lenauer & Riller (2017). In the North Range of the SS, data indicate that the rock units tend to dip mainly in one direction (south), thus lacking the structural complexity for a probable location of a central uplift at depth (Cite Naldrett, 2003).

4.2.2. Multiring Basins

Multiring basins are impact structures that originated from the crash of projectiles that can have an extent of hundreds of kilometers in diameter (French, 1998). They are conformed by concentric uplifted rings and grabens. Generally, in addition to the outer rim of the basin, there are two or more inner rings within the structure (French, 1998). On

Earth, multiring basins are believed to develop at craters with a diameter >100 km, though much of their origin process remains uncertain (French, 1998).

As stated before, nowadays, it is still unclear whether the Sudbury Structure represents a complex crater, a multiring basin, or a structure resulting from a common phase between the formation of these impact structures. However, given the extent of its diameter (≈200-250 km) and the dimension of its SIC, it might be the central portion of a greater complex-multiring crater (French, 1998; Morris et al., 2022).

5. Methods

5.1. Data

To comprehend the structural setting of the Sudbury Structure and examine the location and extent of its possible central uplift, airborne geophysical data were used to analyze the magnetic anomalies present in the basin. This aeromagnetic data, previously used and described by Olaniyan et al. (2013), consists of a merged composite grid with a spatial resolution of 50 m, including existing aeromagnetic data of the Sudbury Structure and part of its surroundings. Table 1 (Olaniyan et al., 2013) summarizes the information relevant to the data sources that form the final grid.

Table 1. Description of airborne geophysical data sets used.

S/No	Data type	Flight height	Flight line spacing	Cell size	Data provided courtesy of
1	Magnetic	43 m	100 m	20 m	Xstrata
2	Magnetic	Variable	200 m	50 m	Geological Survey of Canada
3	Magnetic	Variable	Variable	10 m	Wallbridge Mining

Note. From Qualitative geophysical interpretation of the Sudbury Structure, by Olaniyan et al., 2013, p. T28.

In addition to the aeromagnetic data, several geological and structural data were also used to observe the behavior of the dip and dip direction angles of the Sudbury Structure's bedrock. Table 2 summarizes the types of data used for this endeavor. Dreuse et al. (2010) and Lenauer & Riller (2012) maps can be consulted in Annex 1 and Annex 2, respectively.

Table 2. Description of used geological and structural data sets.

S/No	Data type	File type	Data set description	Data provided courtesy of
1	Geological Structural	Geodatabase	Bedrock base map (1:250.000) with main faults and lineaments	Ontario Geological Survey (2023)
2	Structural	Map	Dip magnitude angles	Dreuse et al.

			for the SIC contacts	(2010)
3	Structural	Map	Foliation directions and dip magnitudes	Lenauer & Riller (2012)
4	Topographic	Raster	Digital Elevation Model (20 m)	ASF Data Search (NASA, 2023)

Finally, information regarding the magnetic susceptibility of the local rocks was compiled through open-source data sets provided by the Ontario Geological Survey (2023). It should be taken into account that although this magnetic susceptibility dataset shows some of the local SS rocks susceptibility measurement, it was impossible to access the same information in this study's critical central zone of interest, so other values from published literature were additionally used (Card et al., 1984; Gupta et al., 1984).

For the SIC, Whitewater Group, and mafic or felsic intrusions, the general susceptibility values varied within defined ranges that correlated to the units' magnetic behavior. For the Noritic units, the susceptibility values mainly ranged between 0,5-0,1 SI to some peak values around 2-3 SI. The values used mainly ranged between 0,1-0,02 for the Quartz Gabbroic units. In the Granophyric units, the susceptibility values ranged from 0,04 SI to almost null magnetic susceptibility estimations. For the Whitewater Group units, the susceptibility values used ranged around 0,05-0,01SI. The susceptibility values used for the mafic and felsic intrusion units were mainly below 0,04 SI. Finally, some negative values were also used between the modeled rock units, but they do not represent the general susceptibility of the area; nevertheless, their inclusion and probable source are discussed in further article sections. The complete list of susceptibility values used can be consulted in Annex S3. The total intensity of the Magnetic Field in the area was 57273 nT, its inclination (deg.) was 73.3, and its declination (deg.) was -9.9 (Alken et al., 2021).

5.2. Geological Modeling of Geophysical Data

Geological modeling of geophysical data is a convenient tool to simulate geological environments' physical and structural characteristics. In this project, 2D and 3D geological models were used to envisage the structural setting of the bedrocks underlying the Sudbury Structure's surface.

2D geological models comprise cross-sections that hold the geological layer's disposition at depth; these 2D sections are delimited by lines that stand for bedrock interface contacts (Anquez et al., 2019). On the other hand, 3D geological models can be made based on a 2D model as a base, following its contours and defined geometry.

The Tensor Research ModelVision software (Tensor Research, 2023) was used to establish the 2D cross-sections over the aeromagnetic map of the area of interest. For this, synthetic lines were deployed in the areas considered crucial for understanding the underlying structural setting of the bedrock. These synthetic lines were later sampled with information on the aeromagnetic grid and a magnetic regional model for the area. This regional magnetic field was calculated to remove long wavelength components of the magnetic field during modeling; this 2D regional is crucial for simultaneously modeling cross-sections of complex anomalies (Tensor Research, 2023). It was possible to model 2D bodies that simulate the magnetic response of the aeromagnetic data shown by the synthetic lines by observing the compiled data in several cross-section diagrams (for a full view of each modeled 2D section, please refer to Annex S4). These 2D bodies generated a simulated magnetic signal that fit the basin's observed magnetic signal. Modeling started with drafting simple tabular bodies with a dip constrained by Dreuse et al. (2010) and Lenauer & Riller's (2012) models. Then, the actual lithological bodies were drafted on top with a similar geometry. One limitation of 2D modeling is that each body must have uniform properties. In reality, the susceptibility distribution of a rock formation follows a broader statistical distribution (Enkin, 2014). In order to simulate that, each unit was split into several parallel bodies with varying susceptibilities, as shown in Figure 4.

After covering with 2D sections the whole area of study, it was possible to observe the cross-sections at depth with the software Leapfrog Geo (Seequent, 2023). Then, using the three-dimensional tools available in this software, it was possible to create 3D lines between the established bedrock's contacts. Then, these lines were correlated with 3D surfaces that interrelated the contacts established by the 2D sections at depth.

6. Results

Magnetic and ancillary structural data for the Sudbury Structure's South Range were compiled from published studies by Dreuse et al. (2010), Lenauer & Riller (2012), and Olaniyan et al. (2013). The structural data sets showed that the dip directions and foliation trajectories of the South Range constantly changed along its margin, sometimes switching abruptly within the same bedrock unit (Dreuse et al., 2010; Lenauer & Riller, 2012). The SIC's dip values ranged from 66-35° to less steep values of 20° approximately, and their dip directions ranged from southeast to northwest plunging (Figure 1). The area that could allow for a better understanding of the bedrock units' behavior was chosen by selecting reliable dip values that defined a considerably changing dip direction area, as this could indicate variations from a just planar stratigraphy of the bedrock units at depth. Within this area, located in the central zone of the South Range, nine synthetic lines were defined as the location for the prospective 2D modeled cross-sections (Figure 1).

Once the location of the synthetic lines was defined, they were drafted in ModelVision software (Tensor Research, 2023). Lines were sampled with information on the Total Magnetic Intensity grid and the calculated regional magnetic field. This allowed the modeling of 2D bodies that simulated the synthetic line's magnetic signal using known structural and magnetic susceptibility data (for further details, refer to Section 5.1). The results were ten 2D cross-sections showing the structural trend of the bedrock units in the area of interest (Figure 4); for a detailed view of each of the modeled cross-sections, please refer to Annex S4.

These 2D cross-sections were later loaded in Leapfrog Geo software to visualize them at depth (Figure 4) and construct 3D surfaces from their defined geometries (Figure 5). The results were five 3D surfaces (see Annex 5 for .DXF files) that represent the contact between the bedrock units, and to facilitate its further analysis, the surfaces were divided into a western (W), a central (C), and an eastern (E) zone (Figure 5).

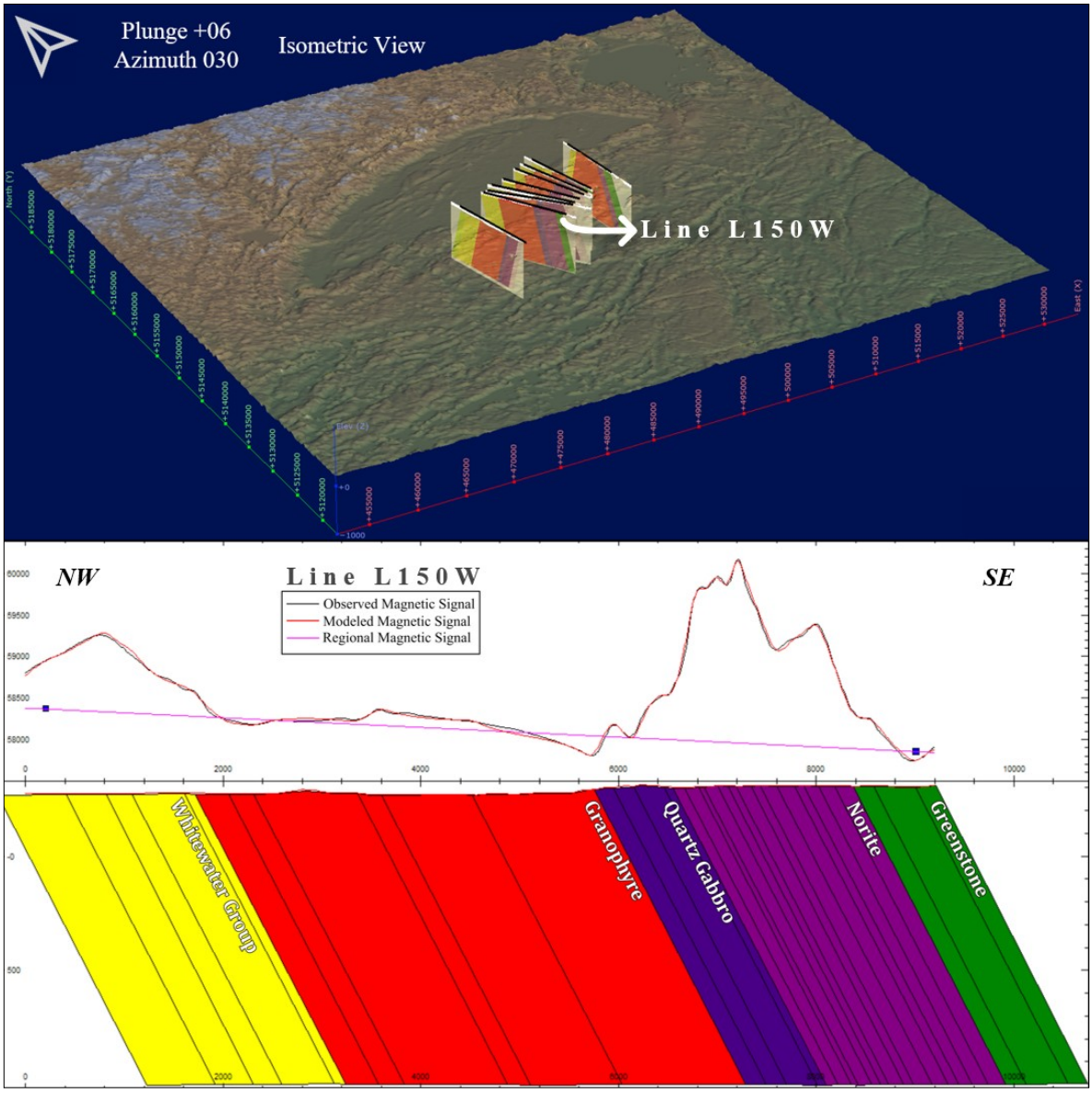

Figure 4. 2D modeled sections for the central area of Sudbury's South Range. Up: Deployment at depth of the 2D sections; the synthetic line L150W has been highlighted. Down: Detailed view of the 2D section corresponding to the synthetic line L150W.

The W zone presents a gently folded tendency that extends across all the modeled surfaces; it initiates (in the southwest of the model) with the surfaces dipping at approximately 45° northwest, and as they extend northeast, their dipping angle reduces to around 30° with a clear dip direction to the southeast (Figure 5, c). The C Zone presents a fold (with its axis pointing northwest) constituted by ≈60° dipping southeast lithologies (Figure 5, b); it is worth noting that this central fold is more evidently deformed at the Noritic surface, whereas in the upper-layer surfaces, it seems to smooth out as it gradually extends to the northern lithologies (Figure 5, d).

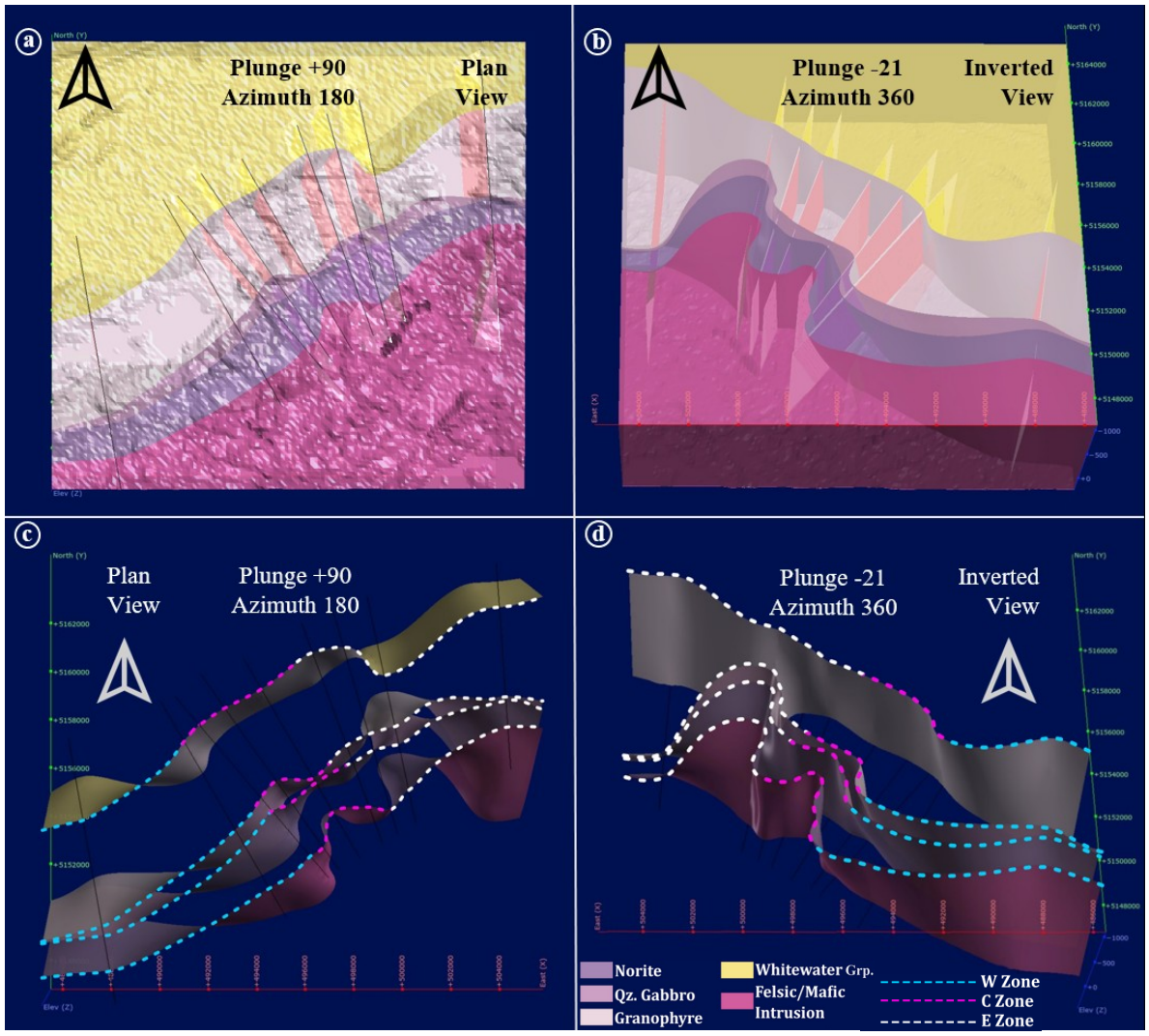

Figure 5. 3D geological model of the Sudbury's South Range central zone. A: Plan view of the geological model (GM), including 3D surfaces, 2D sections, and synthetic line's location; lithologies have been colored. B: Inverted view of the GM, including 3D surfaces, 2D sections, and synthetic line's location; lithologies have been colored. C: Plan view of the GM, including 3D surfaces, synthetic line's location, and Zones division. D: Inverted view of the GM, including 3D surfaces, synthetic line's location, and Zones division.

The E Zone contains another fold clearly defined in the SIC surfaces (i.e., Norite, Quartz Gabbro, and Granophyre contacts), with its axis pointing to the northeast and constituted by ≈38° dipping lithologies (Figure 5, b, d); in the SIC layers, the rocks start pointing northwest once they begin to fold from the C Zone and then change direction to south-southwest as they extend northeast. For the Whitewater Group in the E Zone, the surfaces' northwest direction prevails along its margin, developing an antiform-shaped structure with the south-dipping lithologies of the SIC (Figure 5, d). Finally, it is also worth

noting that right at the contacts between the W, C, and E zones, there are some gently deformed folds with their axis pointing mainly southeast (Figure 5, d).

7. Discussion

This study used a three-dimensional model of the more magnetic data in the Sudbury Structure's South Range's central zone to evaluate whether the impact structure's central uplift could be identified within this area. The modeled 3D surfaces in the final geological model show a structural trend that can be interpreted as the structure's central uplift based on its setting geometry and the structural behavior of the modeled interfaces (Figure 6). Thus, the initial hypothesis that the Sudbury Structure's South Range houses the impact crater's central uplift can be considered a reliable possibility.

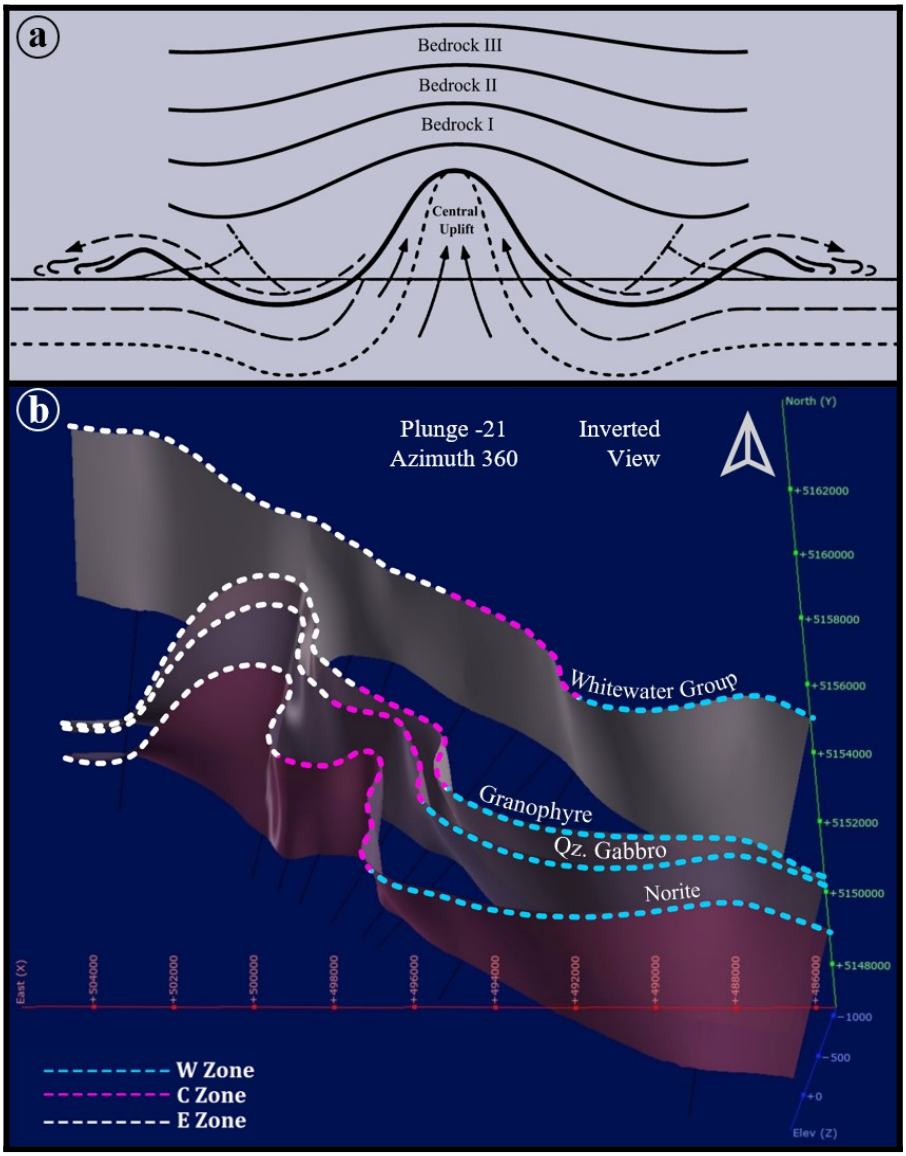

Figure 6. Sudbury Structure's modeled central uplift. A: Conceptual geological model for a present central uplift scenario, modified from Reimold and Koeberl (2014). B: Inverted view of the final 3D model, including 3D surfaces, synthetic line's location, and Zones division.

It is important to remark that this 3D model has been elaborated primarily using the structural data proposed for the Sudbury Basin by Dreuse et al. (2010) and Lenauer & Riller (2012), a Total Magnetic Intensity grid published by Olaniyan et al. (2013) was also used, plus published susceptibility data values by Card et al., (1984), Gupta et al., (1984), and the Ontario Geological Survey (2023). To facilitate its analysis, the 3D surfaces were divided into a western (W), a central (C), and an eastern (E) zone (Figure 6b). As a first approach, the final geological model can be compared with a conceptual geological model showing the expected disposition of the bedrock's units on a present central uplift scenario (Figure 6a). In the conceptual model, it can be seen how the bedrock units tend to fit the emplaced central uplift (Figure 6a, behavior of Bedrock I). At the same time, they gently become shallow as they overlay the units underneath (Figure 6a, behavior of Bedrock III). This same behavior can be seen in the C Zone of the 3D modeled surfaces, as the noritic surface can be considered the layer that houses the central uplift (with its well-defined dome-shaped fold pointing northwest), and the rest of SIC (Quartz Gabbroic and Granophyric surfaces) and Whitewater Group units of the C Zone the overlaying, more horizontal bedrocks that followed the central uplift's formation.

The presence of the central uplift in the SIC's noritic Lower Zone can be correlated with the study of Grieve and Therriault (2000), who suggested that the SIC units might overlay a central uplift. French (1967, 1972, as cited in Rousell, 1984) proposed that after the central uplift's formation, it subsided into the subsurface, which can be counted for what is shown in the model. This structure's presence in the basin's South Range can also be associated with the indications of Gupta et al. (1984) and Lenauer & Riller (2017) that the Sudbury Structure's South Range has been previously uplifted. Additionally, the impact-induced central uplift proposed by Prevec et al. (2005) can be likened to the central uplift structure proposed in our model. Another important notation is that the presence of a central uplift might indicate that the Sudbury Structure represents the central portion of a greater complex crater, though it also might represent a complex-multiring crater given the basin's total diameter (≈200-250 km) (French, 1998; Morris et al., 2022).

It is worth noting that the E Zone also presents a folding structure in the modeled SIC surfaces. Nevertheless, this fold is unlikely to represent the central uplift that's been looked for, as its structural setting does not coincide with the expected disposition shown in

the previously proposed conceptual geological model (Figure 6a). Right at the contact with the C Zone, all the SIC units of the E Zone form a fold in which the axis points northwest and then south without the expected horizontalization occurring; plus, the Whitewater Group units fold at opposite directions of the SIC surfaces, developing an antiform structure rather than a dome-shaped one. It is also worth noting that, in the E Zone, the total density of available data is relatively inferior to that in the rest of the model, dimming the final reliability of this Zone's modeled structural behavior.

The susceptibility data used in the final model includes some negative values corresponding to inner variations within the modeled bedrock units. Also, in this study's final model, the noritic units have the highest susceptibility values, whereas, in estimations made by Gupta et al. (1984), the quartz gabbroic units are stated as the peak susceptibility layers for the SIC units. Not only can this study's final susceptibility data behavior be attributed to inner-composition variations within Sudbury's rock units, but it can also result from the remanent magnetization in the basin's rocks. This remanent magnetization can be considerably high in the SIC units (H.A. Ugalde & W. A. Morris, personal communication, 2023), leading to a significant decay in the observed susceptibility values. The present deformation structures in the area represent another critical factor in the variable susceptibility values across Sudbury's Basin. Future studies regarding magnetic modeling in the area might consider using remanent magnetization data to establish a more detailed outlook on this behavior.

The origin of the SIC has been attributed to crustal melting caused by a meteorite impact (Percival & Easton, 2007). Therefore, and considering that the SIC's noritic Lower Zone was one of the earliest units to have formed during the impact (as stated by the available stratigraphic data (Ontario Geological Survey, 2023)), it is possible to relate the development of the SIC's Lower Zone with the beginning of the central uplift's formation; which could consequently led the Lower Zone to acquire the distinctive dome-shaped geometry seen in the final model.

In summary, the presence of the central uplift in the Sudbury Structure's South Range is supported by the structural disposition of the modeled 3D surfaces in the final model proposed here (Figure 6). This result might be a crucial piece of information for

future ore exploration studies in one of the world's most profitable quarries (i.e., Sudbury's Basin).

Furthermore, developing the presented 3D model improves the understanding of the subsurface South Range's rocks disposition, as it relates some of its main magnetic and structural characteristics to the final modeled surfaces' magnetic values and geometrical tendencies.

8. Conclusions

In this study, a three-dimensional model elaborated with structural and magnetic data for the Sudbury Structure's South Range's central zone was made to evaluate the presence of a central uplift within this area. The result was a geological model consisting of four 3D surfaces that illustrate the structural trends of the bedrock's units present in the area's subsurface. Four main conclusions can be stated from this result:

I. A dome-shaped structure was identified on the noritic interface of the model that can be associated with a central uplift structure. A horizontalizing behavior on the overlaying surfaces supports this deduction.

II. There is a correlation between the SIC's Lower Zone development and the start of the central uplift's formation after the impact that formed the final crater.

III. The presence of a central uplift might indicate that the Sudbury Structure represents the central portion of a greater complex crater, though it also might represent a complex-multiring crater given the basin’s total diameter.

IV. Future studies regarding magnetic modeling in the area might consider using remanent magnetization data to establish a more detailed outlook on the behavior of the bedrock units' magnetic susceptibility.

Finally, identifying the presence of the Sudbury Structure's central uplift in its South Range, as indicated by this study's model, can be a fundamental consideration for future ore exploration in the Sudbury Basin, as it helps clarify the subsurface South Range's rocks disposition, relating some of its main magnetic and structural characteristics to the final modeled surfaces' magnetic values and geometrical tendencies.

9. References

Alken, P., Thébault, E., Beggan, C. D., Amit, H., Aubert, J., Baerenzung, J., Bondar, T. N., Brown, W. J., Califf, S., Chambodut, A., Chulliat, A., Cox, G. A., Finlay, C. C., Fournier, A., Gillet, N., Grayver, A., Hammer, M. D., Holschneider, M., Huder., L., … Zhou, B. (2021). International Geomagnetic Reference Field: the thirteenth generation. *Earth, Planets and Space* 73(49). https://doi.org/10.1186/s40623-020-01288-x

Anquez, P., Pellerin, J., Irakarama, M., Cupillard, P., Lévy, B., & Caumon, G. (2019). Automatic correction and simplification of geological maps and cross-sections for numerical simulations. *Comptes Rendus Geoscience,* 351(1), 48-58. https://doi.org/10.1016/j.crte.2018.12.001

Britannica, The Editors of Encyclopaedia (2023). Canadian Shield. *Encyclopedia Britannica*. October 20. https://www.britannica.com/place/Canadian-Shield.

Card, K. D., Gupta, V. K., McGrath, P. H., & Grant, F. S. (1984). Chapter 2, The Sudbury Structure: Its Regional Geological and Geophysical Setting. In E. G. Pye, A. J. Naldrett, & P. E. Giblin (Eds), *The Geology and Ore Deposits of the Sudbury Structure, Special Volume I* (p. 25). Ontario Geological Survey.

Dietz, R. S. (1964). Sudbury Structure as an Astrobleme. *Journal of Geology*, 72 (p. 412-434).

Dressler, B. O. (1984). Chapter 4, General Geology of the Sudbury Area. In E. G. Pye, A. J. Naldrett, & P. E. Giblin (Eds), *The Geology and Ore Deposits of the Sudbury Structure, Special Volume I* (p. 25). Ontario Geological Survey.

Dressler, B. O., Morrison, G. G., Peredery, W. V., & Rao, B. V. (1987). The Sudbury Structure, Ontario, Canada – A Review. In J. Pohl (Ed.), *Research in terrestrial impact structures* (p. 39). Springer Fachmedien Wiesbaden.

Dreuse, R., Doman, D., Santimano, T., & Riller, U. (2010). Crater floor topography and impact melt sheet geometry of the Sudbury impact structure, Canada. *Terra Nova,* 22(6), 463-469. https://doi.org/10.1111/j.1365-3121.2010.00965.x

Dressler, B. O., Peredery, W. V., & Muir, T. L. (1992). *Geology and mineral deposits of the Sudbury Structure*. Ontario Geological Survey, Guidebook 8.

Enkin, R. J. (2014). The Rock Physical Property Database of British Columbia, and the distinct petrophysical signature of the Chilcotin basalts, *Canadian Journal of Earth Sciences* 51(327-338). http://dx.doi.org/10.1139/cjes-2013-0159

French, B. M. (1998). Traces of Catastrophe: A Handbook of Shock-Metamorphic Effects in Terrestrial Meteorite Impact Structures. LPI Contribution No. 954, Lunar and Planetary Institute, Houston. (p. 120).

Giblin, P. E. (1984). Chapter 1, History of Exploration and Development, of Geological Studies and Development of Geological Concepts. In E. G. Pye, A. J. Naldrett, & P. E. Giblin (Eds), *The Geology and Ore Deposits of the Sudbury Structure, Special Volume I* (p. 3). Ontario Geological Survey.

Grieve, R., & Therriault, A. (2000). Vredefort, Sudbury, Chicxulub: Three of a Kind? *Annual Review of Earth and Planetary Sciences* 28(p. 305-338). https://doi.org/10.1146/annurev.earth.28.1.305

Gupta, V. K., Grant, F. S., Card, K. D. (1984). Chapter 18, Gravity and Magnetic Characteristics of the Sudbury Structure. In E. G. Pye, A. J. Naldrett, & P. E. Giblin (Eds), *The Geology and Ore Deposits of the Sudbury Structure, Special Volume I* (p. 381). Ontario Geological Survey.

Kellet, D. A., Pehrsson, S., Skipton, D. R., Regis, D., Camacho, A., Schneider, D. A., & Berman, R. (2020). Thermochronological history of the Northern Canadian Shield. *Precambrian Research*, 342(105703). https://doi.org/10.1016/j.precamres.2020.105703.

Kenkmann, T., Jahn, A., Scherler, D., & Ivanov, B. A. (2005). Structure and formation of a central uplift: A case study at the Upheaval Dome impact crater, Utah. In T. Kenkmann, F. Hörz, & A. Deutsch (Eds.), *Large Meteorite Impacts III* (p. 85). Geological Society of America. https://doi.org/10.1130/0-8137-2384-1.85

Lenauer, I., & Riller, U. (2012). Strain fabric evolution within and near deformed igneous sheets: The Sudbury Igneous Complex, Canada. *Tectonophysics* 558-559(p. 45-57). https://doi.org/10.1016/j.tecto.2012.06.021

Lenauer, I., & Riller, U. (2017). A trishear model for the deformation of the Sudbury Igneous Complex, Canada. *Journal of Structural Geology* 97(p. 212-224). http://dx.doi.org/10.1016/j.jsg.2017.03.006

Milkereit, B., Artemieva, N., & Ugalde, H. (2008). Geophysical signature of the footwall of large meteorite impact craters. In *Large Meteorite Impacts and Planetary Evolution IV* (p. 152). LPI Contribution No. 1423, Lunar and Planetary Institute, Houston.

Mira Geoscience. (2023). *Geoscience ANALYST* [Computer software]. Retrieved from https://mirageoscience.com/mining-industry-software/geoscience-analyst/

Morris, W. A., Underhay, S. L., & Ugalde, H. (2022). Morphology and tectonic modification of the Sudbury impact crater: the North Range. *Canadian Journal of Earth Sciences,* 60(7), 974-988. https://doi.org/10.1139/cjes-2022-0066

Mugiraneza, S., & Hallas, A. M. (2022). Tutorial: a beginner's guide to interpreting magnetic susceptibility data with the Curie-Weiss law. *Communications Physics,* 5(95). https://doi.org/10.1038/s42005-022-00853-y

Muir, T. L. (1984). Chapter 21, The Sudbury Structure: Considerations and Models for an Endogenic Origin. In E. G. Pye, A. J. Naldrett, & P. E. Giblin (Eds), *The Geology and Ore Deposits of the Sudbury Structure, Special Volume I* (p. 449). Ontario Geological Survey.

Naldrett, A. J. (1984). Introduction to the Geology of the Sudbury Igneous Complex. In E. G. Pye, A. J. Naldrett, & P. E. Giblin (Eds), *The Geology and Ore Deposits of the Sudbury Structure, Special Volume I* (p. 234). Ontario Geological Survey.

Naldrett, A. J. (2003). From Impact to Riches: Evolution of Geological Understanding as Seen at Sudbury, Canada. *GSA Today* 13(p. 4-9). http://dx.doi.org/10.1130/1052-5173(2003)013%3C0004:FITREO%3E2.0.CO;2

NASA. (2023). *ASF Data Search Vertex. https://search.asf.alaska.edu/#/?zoom=3.000&center=-97.494,39.673*

Olaniyan, O., Smith, R. S., & Morris, B. (2013). Qualitative geophysical interpretation of the Sudbury Structure. *Interpretation,* 1(1), T25-T43. http://dx.doi.org/10.1190/INT-2012-0010.1

Ontario Geological Survey. (2023). OGSEarth. https://www.geologyontario.mndm.gov.on.ca/ogsearth.html

Percival, J.A., & Easton, R.M. (2007). *Geology of the Canadian Shield in Ontario: an update* (Open File Report 6196). Ontario Geological Survey. https://www.google.com/url?

sa=t&rct=j&q=&esrc=s&source=web&cd=&ved=2ahUKEwjikJ_uzpKCAxWNm2oFHY5IBCoQFnoECAkQAQ&url=http%3A%2F%2Fwww.geologyontario.mndm.gov.on.ca%2Fmndmfiles%2Fpub%2Fdata%2Fimaging%2Fofr6196%2FOFR6196.pdf&usg=AOvVaw13-TkiReFfenLxdmw6-UD5&opi=89978449

Peredery, W. V., & Morrison, G. G. (1984). Chapter 22, Discussion of the Origin of the Sudbury Structure. In E. G. Pye, A. J. Naldrett, & P. E. Giblin (Eds), *The Geology and Ore Deposits of the Sudbury Structure, Special Volume I* (p. 491). Ontario Geological Survey.

Prevec, S. A., Cowan, D. R., Cooper, G. R. J. (2005). Geophysical evidence for a pre-impact Sudbury dome, southern Superior Province, Canada. *Canadian Journal of Earth Sciences* 42(p. 1-9). https://doi.org/10.1139/e04-097

Reimold, W.U., Koeberl, C. (2014). Impact structures in Africa: A Review. *Journal of African Earth Sciences*. doi: http://dx.doi.org/10.1016/j.jafrearsci.2014.01.008

Renwick, W. H. (2009). Lakes and Reservoirs of North America. In G. E. Likens (Eds), *Encyclopedia of Inlad Waters* (p. 524-532). Academic Press. https://doi.org/10.1016/B978-012370626-3.00033-8.

Riller, U. (2005). Structural characteristics of the Sudbury impact structure, Canada: Impact-induced versus orogenic deformation—A review. *Meteoritics & Planetary Science,* 40(11), 1723-1740. https://doi.org/10.1111/j.1945-5100.2005.tb00140.x

Rousell, D. H. (1984). Chapter 8, Onwatin and Chelmsford Formations. In E. G. Pye, A. J. Naldrett, & P. E. Giblin (Eds), *The Geology and Ore Deposits of the Sudbury Structure, Special Volume I* (p. 211). Ontario Geological Survey.

Seequent. (2023). *Leapfrog Geo 5.0* [Computer software]. Retrieved from https://www.seequent.com/es/productos-y-soluciones/leapfrog-geo/

Stockwell, C.H. (1975). *World Regional Geology. Encyclopedia of Earth Science*. Springer, Berlin, Heidelberg. https://doi-org.ezproxy.eafit.edu.co/10.1007/3-540-31081-1_24

Tensor Research. (2023). *ModelVision* [Computer software]. Retrieved from https://www.tensor-research.com.au/

Annexes' Link

https://drive.google.com/drive/folders/1njxLgqySJ9aVAUpHzyE57vl3ZJQ68jmx?usp=drive_link